Turkish Journal of Physics

Volume 39 | Number 3 Article 4

1-1-2015

Solution processable graphene oxide hole transport layers and their application in P3HT:HHPER active layer based BHJSCSolution processable graphene oxide hole transport layers and their application in P3HT:HHPER active layer based BHJSC

GÖRKEM MEMİŞOĞLU

HALİDE DİKER

CANAN VARLIKLI

Turkish Journal of Physics

http://journals.tubitak.gov.tr/physics/

Research Article

Turk J Phys
(2015) 39: 254 – 263

doi:10.3906/fiz-1504-5

Solution processable graphene oxide hole transport layers and their application in P3HT:HHPER active layer based BHJSC

Görkem MEMİŞOĞLU[1,2], **Halide DİKER**[1,3], **Canan VARLIKLI**[1,*]
[1]Solar Energy Institute, Ege University, Bornova, İzmir, Turkey
[2]Vestel Electronics, MOS, Manisa, Turkey
[3]Dyo Boya Fab. San. Tic. A.Ş., AOSB Çiğli, İzmir, Turkey

Received: 12.04.2015 • **Accepted/Published Online:** 18.06.2015 • **Printed:** 30.11.2015

Abstract: Graphene oxide (GO) material was synthesized by an improved Hummers method and characterized by FT-IR, XPS, XRD, AFM, SEM, and UV-VIS analyses. The thickness of the GO layer was measured as 1.5 nm. Solution processed bulk heterojunction solar cells comprising poly(3-hexylthiophene) (P3HT) as the electron donor and N,N'-bis-2-(1-hydoxyhexyl)-3,4,9,10-perylenebis(dicarboximide) (HHPER) as the electron acceptor component of the active layer were produced with and without the GO doped PEDOT-PSS hole transport layers. The optical investigations of the active layer were performed by ground state absorption and photoluminescence measurements. Optimized blend w/w was determined as P3HT:HHPER, 3:1. It was found that the presence of GO in PEDOT:PSS by 0.05 w/w reduces the charge transfer resistance and enhances not only the J_{sc}, but also V_{oc} values. However, it cannot inhibit V_{oc} losses obtained through annealing the active layer at temperatures higher than 120 °C.

Key words: Bulk heterojunction solar cell, perylenediimide, graphene oxide, impedance spectroscopy

1. Introduction

Oxidation of graphite was achieved for the first time by Brodie in 1859 [1] and the method applied was improved by using H_2SO_4 in 1898 [2]. In 1958 Hummers and Offman tried a new approach to oxidize graphite [3] and Tour et al. prepared graphene oxide (GO) by using $KMnO_4$, H_2SO_4, and H_3PO_4 in the oxidation reaction and referred to their process as the "improved Hummers method" [4]. GO consists of a graphene sheet with carboxylic acid, ketone, and ester groups at the edge, epoxy, and hydroxyl groups on the basal plane [5]. Because of these functional groups, GO is able to go into both physical and chemical interactions with the secondary additives [6,7].

The solution processed bulk heterojunction solar cell (BHJSC) is a promising photovoltaic technology [8–10]. There are lots of studies based on the active layer of poly(3-hexylthiophene) (P3HT) and methanofullerene, [6,6]-phenyl C61-butyric acid methyl ester (PCBM) blends. Although PCBM is widely used, because of its high cost and difficult synthetic requirements, alternative electron acceptor material investigations are carried out. Perylenediimides (PDIs) are considered as one of the potential material types due to their high absorption coefficients, high thermal stability, and relatively good electron acceptor properties [11–15]. In the first part of this study, a PDI derivative, i.e. N,N'-bis-2-(1-hydoxyhexyl)-3,4,9,10-perylenebis(dicarboximide) (HHPER), is substituted with PCBM and used as the n-type component of a BHJSC.

*Correspondence: canan.varlikli@ege.edu.tr

Poly(3,4-ethylenedioxythiophene):poly(styrenesulfonate) (PEDOT-PSS) is widely used as hole transport layer (HTL) in organic optoelectronic devices. Although its acidic nature causes some deficiencies like etching the transparent conductive oxide (TCO) surface, its advantages such as smoothing the ITO surface and creating good contact between the ITO and other layers make it almost indispensable [16]. In the last few years GO has started to be considered as an HTL alternate. However, there are some difficulties with full coverage of GO on an ITO substrate, and therefore it is most of the time applied as an interconnect HTL layer: PEDOT-PSS:GO blends. According to the literature, PEDOT-PSS:GO blends present higher solar energy conversion efficiencies than that of the pristine PEDOT-PSS [17,18]. In the second part of this study, GO doped PEDOT-PSS HTLs with a doping ratio of 0.05 w/w are used as the hole extraction electrodes of the BHJSC with the active layer of the P3HT:HHPER blend.

2. Experimental

2.1. Materials

Graphite powders, potassium permanganate ($KMnO_4$), sulfuric acid (H_2SO_4), phosphoric acid (H_3PO_4), and hydrogen peroxide (H_2O_2) were obtained from Merck. Indium tin oxide (ITO) coated glass substrates were obtained from Delta Technologies (4–10 $\Omega/\square$). Glass slides (quartz) were obtained from GianTek Quartz (Linyi). Poly(3,4-ethylenedioxythiophene):poly(styrenesulfonate) (PEDOT:PSS) (AL4083), poly(3-hexylthiophene) (P3HT), lithium fluoride (LiF), and aluminum (Al) were purchased from Sigma-Aldrich. HHPER was synthesized according to the literature [13]. All other chemicals used were in analytical grade and used as received.

2.2. Instruments

Absorptions and photoluminescence spectra of thin films were obtained with Analytic Jena S600 UV and Edinburgh FLS920P Spectrophotometers, respectively. Solution processed layer coatings were prepared by a Laurell WS-400B-6NPP-LITE spin coater. The film thicknesses and morphologies of the films were measured by Ambios XP-1 high resolution surface profiler and Ambios Q Scope 250 model atomic force microscope (AFM), respectively. LiF and Al deposition was performed with a shadow mask by a vacuum evaporator that contained a crystal oscillator for thickness measurements and was attached to an MBRAUN 200B glove box system. Keithley 2400 source meter and IM6 Zahner Elektrik impedance analyzer were used for determination of current density–voltage (J–V) and impedance characteristics of the solar cells, respectively. Illumination was provided from an AM 1.5 filter containing a solar simulator attached to the glove box system and the intensity was measured by Nova II versatile laser power energy display that contained a calibrated silicon photodiode. Solar simulator irradiation was fixed to 100 mW/cm^2 at 25 °C.

2.3. Synthesis of GO

Tour's method was applied [4]. Shortly, graphite powders were oxidized by $KMnO_4$ in the 9:1 mixture of concentrated H_2SO_4/H_3PO_4 media at 50 °C for 12 h. The reaction mixture was then cooled to room temperature (RT) and the reaction was terminated by 30% H_2O_2 into ice water. Several filtration, centrifugation and washing steps were repeated for removing the remained solid materials. Finally, GO suspension was filtrated and vacuum-dried overnight at RT.

2.4. Sample preparation for optical investigations

Quartz substrates were cleaned by the general method [19,20]. Before coating the organic layers, they were treated with O_2 plasma for 5 min at 60 W. P3HT (10 mg/mL) and HHPER (10 mg/mL) were dissolved in chlorobenzene and P3HT:HHPER blends with different w/w (4:1, 3:1, 2:1, 1:1, 1:2, and 1:3) were coated on quartz substrates at 1500 rpm.

2.5. Device preparation for electrical investigation

BHJSCs were prepared in the structure of ITO/HTL/active layer/LiF/Al. ITO substrates were etched and cleaned by the general method [19,20] and O_2 plasma treated for 5 min at 60 W. Pristine PEDOT:PSS and PEDOT:PSS doped with 0.05 w/w GO were used as the HTL. This layer was spin-coated at 3000 rpm for 1 min and vacuum dried at 100 °C for 30 min, which resulted in a film thickness of 45 nm. The active layer ($\cong$100 nm) was prepared with P3HT:HHPER (3:1) and annealed at 120 °C, 150 °C, and 180 °C for 15 min in a vacuum oven. Finally, the LiF/Al (0.8 nm/80 nm) electrode was evaporated with a depositing rate of 0.5 Å/s at 3 $\times$ 10^{-6} mbar pressure. The active area of solar cells was 12 mm^2, and five parallel measurements were performed for each device. The energy level diagram of the studied BHJSC is shown in Figure 1 together with the open structures of P3HT and HHPER materials.

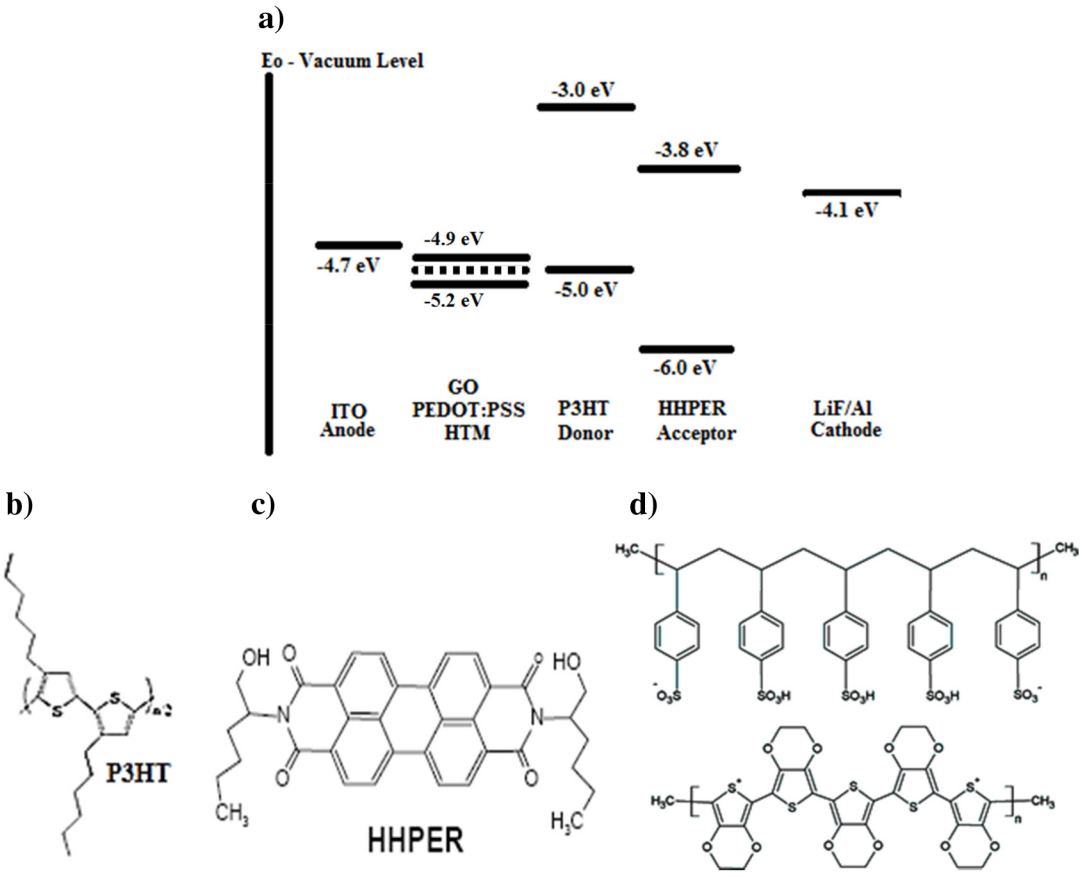

Figure 1. a) Energy level diagram of the studied BHJSC. Chemical structures of: b) P3HT; c) HHPER; and d) PEDOT-PSS.

3. Results and discussion

3.1. Characterization of GO

Characterization results of GO demonstrated that graphite was efficiently oxidized. XRD peaks of precursor graphite and GO were determined at 26.40° (2θ) and 10.15° (2θ), respectively (Figure 2a). These peaks are compatible with the characteristic reflections of graphite (002) and GO (001) [21–23]. Interlayer distances (d-space) are defined as 3.36 Å for graphite and as 8.63 Å for GO. The d-space increment is attributed to the incorporation of oxygen containing functional groups into the carbon lattice [22,24].

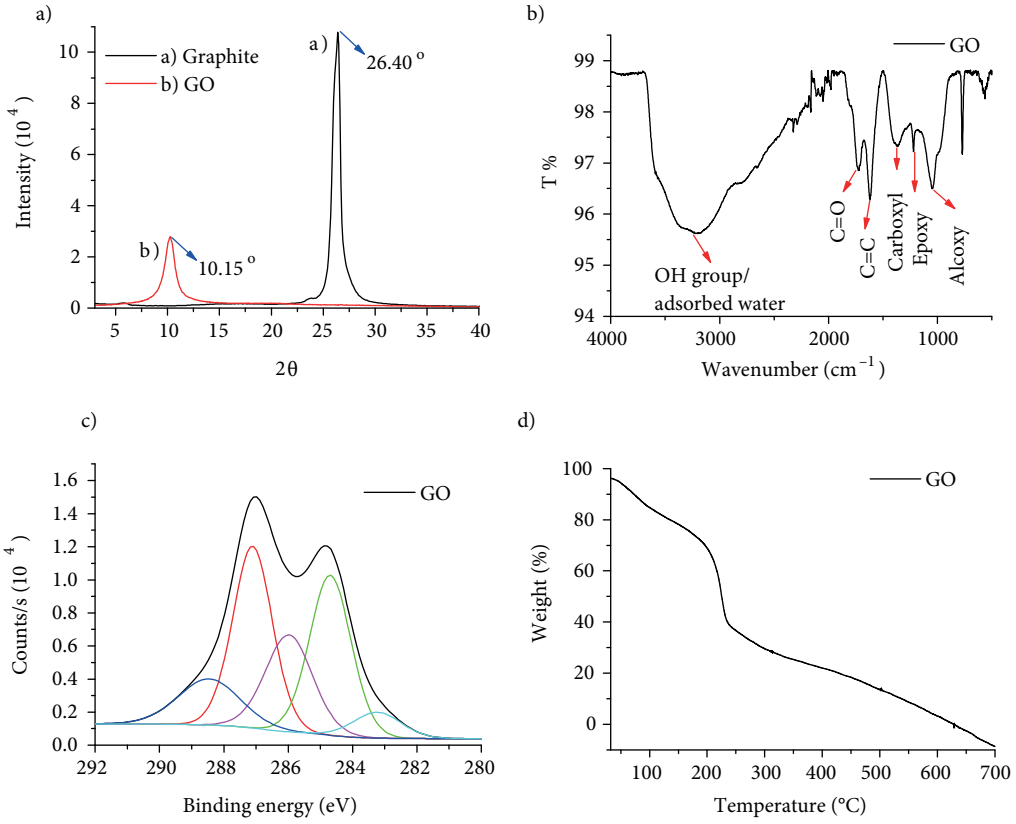

Figure 2. Characterization result: a) XRD spectra of graphite and GO; b) FT-IR spectrum of GO; c) XPS spectrum of GO; and d) TGA curve of GO.

The FT-IR spectrum is presented in Figure 2b. Results confirm the existence of OH ($\sim$3400 cm^{-1}), C-OH (1039 cm^{-1}), C-O-C (1201 cm^{-1}), C=O (1720 cm^{-1}), and C-O of carboxylic acid (1373 cm^{-1}) functional groups in the structure. The peak at 1622 cm^{-1} is related to unoxidized graphitic carbon (C=C) [25–28]. The presence of those functional groups is further confirmed with the XPS analysis (Figure 2c). Five characteristic peaks that are related to sp^2 carbon (C=C, 283.36 eV), sp^3 carbon (C-C, 284.80 eV), epoxy/hydroxyl groups (C-O, 285.98 eV), carbonyl groups (C=O, 287.10 eV), and carboxyl groups (O-C=O, 288.51 eV) are identified from C(1s) binding energy [29–31]. The C:O ratio is determined as 1.94 from the XPS survey spectrum of GO solid samples.

GO is a thermally unstable material. The TGA result for GO is illustrated in Figure 2d. The mass loss ($\cong$ 12%) observed until 100 °C is related to the loss of adsorbed water due to the hygroscopic nature of GO. Significant mass loss ($\cong$40%) is detected at around 200 °C, which is attributable to pyrolysis of oxygen functional groups [32,33].

UV-VIS spectra of GO presented a main absorption peak at 230 nm and a shoulder at approximately 300 nm (Figure 3a). The main peak is related to the $\pi \rightarrow \pi^*$ transition of the aromatic C-C bonds, whereas the latter is related to the n$\rightarrow \pi^*$ transition that is generated from the nonbonding electrons of oxygenated functional groups [23,34]. Figure 3b presents photoluminescence spectrum of GO. Two major emission peaks at 400 nm and 460 nm and small shoulders in the range of 530–650 nm are obtained (λ_{ex}; 230 nm). Those results are in good accordance with the literature [35,36].

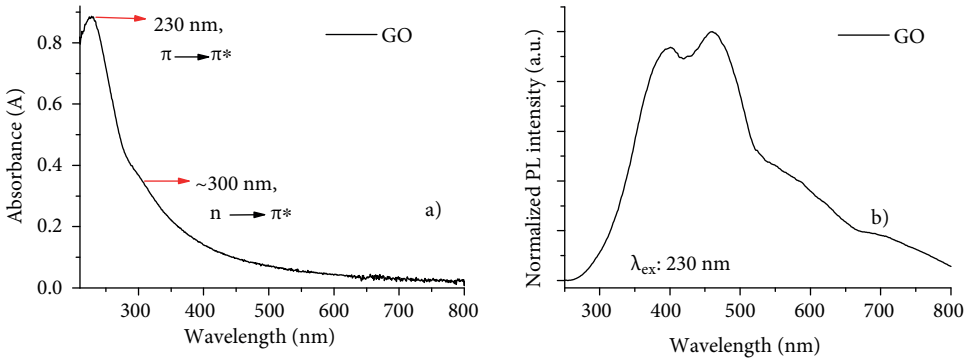

Figure 3. Optical analysis for GO: **a)** UV-VIS absorption spectrum; and **b)** photoluminescence spectrum of GO.

Monolayer graphene sheet is known to have a thickness of 0.34 nm. The GO sheet synthesized in this study has a thickness of 1.5 nm (Figure 4a). The reason for this big difference comes from the functional groups on the basal plane of GO [37,38]. Additionally, wrinkle morphology of the GO that is originated from oxygen functionalities is detected from SEM images of bulk GO sheets (Figure 4b).

3.2. Optical studies and BHJSC performances

PDIs are generally named as pigments rather than dyes because of their limited solubility in regular organic solvents. However, the solubility of the PDI derivative used in this study, i.e. HHPER, allows its utilization in solution processed coatings. As seen in Figure 5a, P3HT and HHPER films present absorptions at almost the same wavelength range. As stated above, the films of those two photosensitizers were prepared from the same stock solution concentrations and were spin-coated at the same rpms. Therefore, one may conclude that the molar absorptivity constant of P3HT is higher than that of HHPER. Nevertheless, increasing the w/w of HHPER in the P3HT:HHPER blend was also tried and the result was as expected: a reduction in the absorption intensity with an increase in HHPER w/w (1:1 to 1:3). However, the absorption intensity of P3HT:HHPER films was enhanced by increasing the P3HT ratio in the blend. Although the absorption intensity of the pristine P3HT film was the highest, the absorbance of HHPER was enhanced by the addition of P3HT. Maximum absorption values in the P3HT:HHPER blends were achieved with blend compositions of 4:1 and 3:1, with no spectral shifts. No matter what the w/w of HHPER in the blend, photoluminescence (PL) quenching was observed. The PL intensity of P3HT was significantly quenched (approximately 90%) in the blend with the 3:1 w/w (Figure 5b). Therefore, P3HT:HHPER (3:1) was determined to be used as the active layer in the BHJSC device structure.

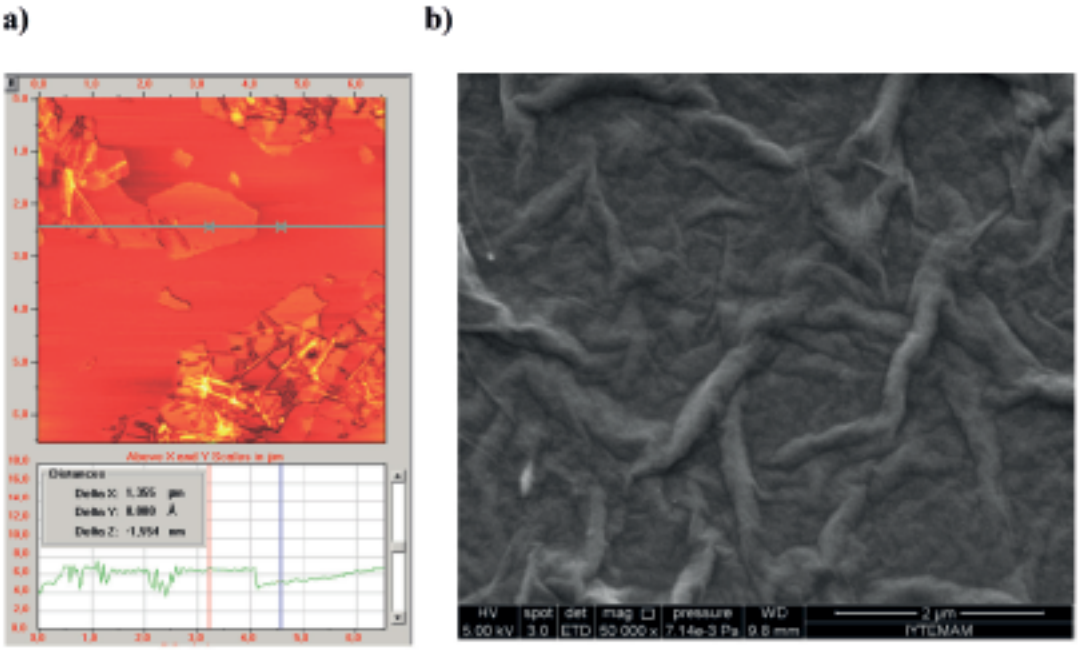

Figure 4. Microscopic analysis of GO: a) AFM image; and b) SEM image.

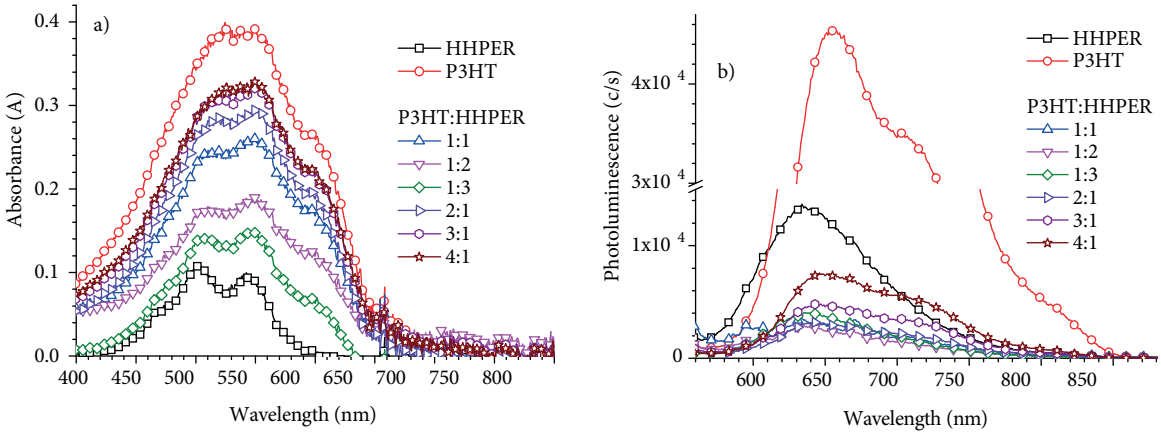

Figure 5. a) Absorption; and b) photoluminescence characteristics of thin films on quartz substrates annealed at 120 °C (λ_{exc} = 540 nm).

P3HT:HHPER (3:1) based BHJSCs were produced in a conventional configuration (ITO/HTL/Active Layer/LiF/Al). The energy diagram of the BHJSC is shown in Figure 1a. The values of the highest occupied molecular orbital (HOMO) and lowest unoccupied molecular orbital (LUMO) of P3HT, HHPER, and work function of GO were taken from literature [14,39,40]. The obtained current density–voltage (J–V) curves (Figure 6a and 6b) presented regular diode behavior and impedance curves (Figure 7) indicated a parallel resistance–capacitance circuit with a single relaxation time, in accordance with the literature [41]. Collected data are summarized in the Table.

Table. Photovoltaic and electrical performances of BHJSCs.

P3HT:HHPER Anneal. temp.	Sample	J_{sc} (mA/cm^2)	V_{oc} (mV)	FF	η	R_s (Ω)	R_p (kΩ)
120 °C	AL4083	0.46 ± 0.04	680 ± 2 5.23	0.28 ± 0.009	0.09 ± 0.01	89.1	5.4
	AL4083 + 0.05 mg/mL GO	0.62 ± 0.06	740 ± 0.00	0.28 ± 0.005	0.13 ± 0.01	87.2	4.5
150 °C	AL4083	0.40 ± 0.03	653 ± 27.1	0.28 ± 0.01	0.07 ± 0.009	97.5	9.6
	AL4083 + 0.05 mg/mL GO	0.45 ± 0.09	545 ± 25.15	0.29 ± 0.003	0.07 ± 0.014	93.7	7.4
180 °C	AL4083	0.61 ± 0.07	200 ± 27.12	0.31 ± 0.027	0.04 ± 0.008	98.3	18.4
	AL4083 + 0.05 mg/mL GO	0.63 ± 0.14	347 ± 24.1	0.33 ± 0.034	0.07 ± 0.004	95.4	11.4

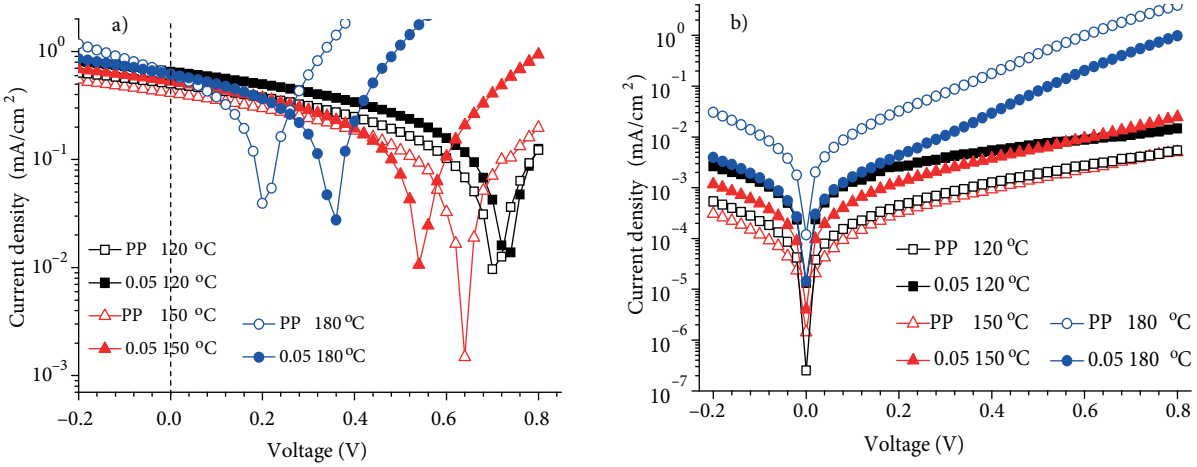

Figure 6. Current density–voltage curves of BHJSCs: a) under 100 mW/cm^2 AM 1.5; and b) in dark.

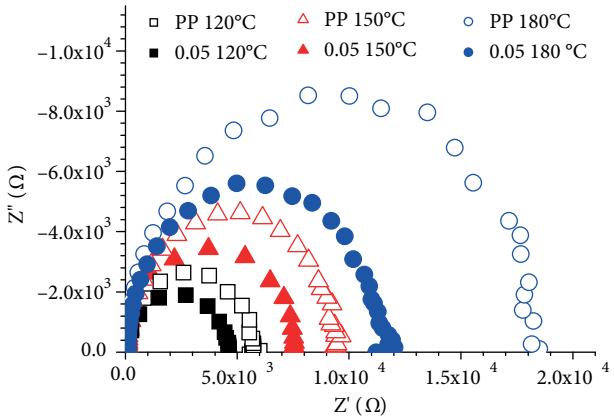

Figure 7. Impedance curves of BHJSCs under 100 mW/cm^2 AM 1.5.

The effect of annealing temperature on BHJSCs that contain P3HT:PCBM blends as the active layer is widely studied in the literature and it is known that annealing of the active layer at around 120 °C, which is below the melting temperature (T_m) of P3HT [42,43], results in better photo conversion efficiency (PCE). The tendencies of short circuit current density (J_{sc}) and open circuit voltage (V_{oc}) values obtained in this study are

in accordance with this fact; shifting the acceptor from PCBM to HHPER did not change addressing 120 °C as the optimum annealing temperature for P3HT based BHJSCs (Table). One may find contradictory reports in the literature that address the possible chemical degradation of the N-alkyl chains of PDI derivatives as the reason for the low efficiency obtained at high annealing temperatures [44]. The generally acknowledged two reasons are: 1) the physical change occurring at the P3HT polymeric chain, and 2) the possible phase segregation between the P3HT and the acceptor molecule that will reduce the donor–acceptor interphase [15,41,42]. The dramatic V_{oc} decrease obtained from the solar cell annealed at 180 °C points out that the energy difference between the LUMO of HHPER and HOMO of P3HT is affected. The parallel resistance (R_p) values confirm this situation. R_p generates from the active layer of a BHJSC and the values of R_p for the annealing temperatures of 120 °C, 150 °C, and 180 °C are 5.4 kΩ, 9.6 kΩ, and 18.5 kΩ, respectively. Moreover, increasing the annealing temperature causes a slight increase in the J_{sc} values. The tendencies of V_{oc} and J_{sc} values show that there may not be a phase segregation happening in the active layer, but the main reason for the PCE decrease is the physical change that the P3HT polymeric chain undergoes with increased annealing temperatures.

The highest PCE that could be achieved with the BHJSC with the configuration of ITO/PEDOT:PSS(Al4083)/P3HT:HHPER (3:1)/LiF/Al was 0.09%. The active layer of this device was annealed at 120 °C. Although there are higher PCE values reported with the use of bay-substituted PDI derivatives as n-type components of the active layer [11,15], this value is comparable with those of the P3HT:N-alkyl substituted PDI in the literature [12,15,39].

No matter what the annealing temperature is, the presence of GO in the PEDOT:PSS layer enhanced the efficiency values. GO has a work function of 4.9 eV [40] and this value is widely accepted as 5.2 eV for PEDOT:PSS. Slight reductions obtained at the serial resistance (Rs) values are apprised as better alignment of the hole collection energy states [18]. It was found that the presence of GO in PEDOT:PSS by 0.05 w/w reduces the charge transfer resistance and enhances not only the J_{sc}, but also the V_{oc} values. It cannot, however, inhibit V_{oc} losses obtained through annealing the active layer at temperatures higher than 120 °C (Table).

4. Conclusion

In this study a PDI derivative was studied as an n-type material alternate to PCBM in a P3HT based BHJSC, and it presented a PCE of 0.09%. An annealing temperature of 120 °C was determined as optimal for P3HT based devices. PCE was further increased to 0.13% by the use of GO as a dopant in the PEDOT:PSS hole transport layer. The used GO dopant w/w was 0.05. This result is promising and further investigations on the GO w/w in PEDOT:PSS are in progress.

Acknowledgments

The authors are thankful to Prof Dr Sıddık İçli, who retired from the Ege University Solar Energy Institute (EU-SEI) in 2014 and made valuable contributions to the organic electronics research infrastructure of EU-SEI. This work was supported by research project funds from the Scientific and Technological Research Council of Turkey (TÜBİTAK) (Project #: 114M508).

References

[1] Brodie, B. C. *Philos. Trans. R. Soc. London* **1859**, *149*, 249–259.

[2] Staudenmaier, L. *Berichte Der Dtsch. Chem. Gesellschaft* **1898**, *31*, 1481–1487 (in German).

[3] Hummers, W. S.; Offeman, R. E. *J. Am. Chem. Soc* **1958**, *80*, 1339.

[4] Marcano, D. C.; Koynkin, D. V.; Berlin, J. M.; Sinitskii, A.; Sun, Z.; Slesarev, A.; Alemany, L. B.; Lu, W.; Tour, J. M. *ACS Nano* **2010**, *4*, 4806–4814.

[5] Lerf, A.; He, H.; Forster, M.; Klinowski, J. *J. Phys. Chem. B* **1998**, *102*, 4477–4482.

[6] Georgakilas, V.; Otyepka, M.; Bourlinos, A. B.; Chandra, V.; Kim, N.; Kemp, K. C.; Hobza, P.; Zboril, R.; Kim, K. S. *Chem. Rev.* **2012**, *112*, 6156–3214.

[7] Mao, H. Y.; Lu, Y. H.; Lin, J. D.; Zhong, S.; Wee, A. T. S.; Chen, W. *Prog. Surf. Sci.* **2013**, *88*, 132–159.

[8] Brabec, C. J.; Sariciftci, S. N.; Hummelen, J. C. *Adv. Funct. Mater.* **2001**, *11*, 15–26.

[9] Gomez De Arco, L.; Zhang, Y.; Schlenker, C. W.; Ryu, K.; Thompson, M. E.; Zhou, C. *ACS Nano* **2010**, *4*, 2865–2873.

[10] Burroughes, J. H.; Bradley, D. D. C.; Brown, A. R.; Marks, R. N.; Mackay, K.; Friend, R. H.; Burns, P. L.; Holmes, A. B. *Nature* **1990**, *347*, 539–541.

[11] Liu, X.; Cai, P.; Chen, D.; Chen, J.; Su, S.; Cao, Y. *Sci. China Chem.* **2014**, *57*, 973–981.

[12] Kamm, V.; Battagliarin, G.; Howard, I. A.; Pisula, W.; Mavrinskiy, A.; Li, C.; Müllen, K.; Laquai, F. *Adv. Energy Mater.* **2011**, *1*, 297–302.

[13] Zafer, C.; Karapire, C.; Sariciftci, S. N.; Icli, S. *Sol. Energy Mater. Sol. Cells* **2005**, *88*, 11–21.

[14] Karapire, C.; Zafer, C.; İçli, S. *Synth. Met.* **2004**, *145*, 51–60.

[15] Kozma, E.; Kotowski, D.; Luzzati, S.; Catellani, M.; Bertini, F.; Famulari, A.; Raos, G. *RSC Adv.* **2013**, *3*, 9185–9188.

[16] Memisoglu, G.; Varlikli, C. *IEEE Photonics Technol. Lett.* **2015**, *27*, 537–540.

[17] Tung, V. C.; Kim, J.; Cote, L. J.; Huang, J. *J. Am. Chem. Soc.* **2011**, *133*, 9262–9265.

[18] Yu, J. C.; Jang, J. I.; Lee, B. R.; Lee, G. W.; Han, J. T.; Song, M. H. *ACS Appl. Mater. Interfaces* **2014**, *6*, 2067–2073.

[19] Memisoglu, G.; Varlikli, C. *Inter. J. Photoen.* 2012, *2012*, 1–11.

[20] Memisoglu, G.; Varlikli, C.; Diker, H. *J. Electron. Mater.* **2013**, *42*, 3502–3511.

[21] Jeong, H. K.; Noh, H. J.; Kim, J. Y.; Jin, M. H.; Park, C. Y.; Lee, Y. H. *EPL (Europhysics Lett.)* **2008**, *82*, 67004–67009.

[22] Wojtoniszak, M.; Chen, X.; Kalenczuk, R. J.; Wajda, A.; Łapczuk, J.; Kurzewski, M.; Drozdzik, M.; Chu, P. K.; Borowiak-Palen, E. *Colloids Surfaces B* **2012**, *89*, 79–85.

[23] Chen, J.; Yao, B.; Li, C.; Shi, G. *Carbon N. Y.* **2013**, *64*, 225–229.

[24] Chen, C.; Yang, Q. H.; Yang, Y.; Lv, W.; Wen, Y.; Hou, P. X.; Wang, M.; Cheng, H. M. *Adv. Mater.* **2009**, *21*, 3007–3011.

[25] Si, Y.; Samulski, E. T. *Nano Lett.* **2008**, *8*, 1679–1682.

[26] Marcano, D. C.; Kosynkin, D. V; Berlin, J. M.; Sinitskii, A.; Sun, Z. Z.; Slesarev, A.; Alemany, L. B.; Lu, W.; Tour, J. M. *ACS Nano* **2010**, *4*, 4806–4814.

[27] Thakur, S.; Karak, N. *Carbon N. Y.* **2012**, *50*, 5331–5339.

[28] Dey, R. S.; Hajra, S.; Sahu, R. K.; Raj, C. R.; Panigrahi, M. K. *Chem. Commun.* **2012**, *48*, 1787–1789.

[29] Wang, D. W.; Du, A.; Taran, E.; Lu, G. Q.; Gentle, I. R. *J. Mater. Chem.* **2012**, *22*, 21085–21091.

[30] Dreyer, D. R.; Park, S.; Bielawski, C. W.; Ruoff, R. S. *Chem. Soc. Rev.* **2010**, *39*, 228–240

[31] Fan, Z. J.; Kai, W.; Yan, J.; Wei, T.; Zhi, L. J.; Feng, J.; Ren, Y. M.; Song, L. P.; Wei, F. *ACS Nano* **2011**, *5*, 191–198.

[32] Qiu, Y.; Guo, F.; Hurt, R. K. *Carbon N Y* **2014**, *72*, 215–223.

[33] Stankovich, S.; Dikin, D. A.; Piner, R. D.; Kohlhaas, K. A.; Kleinhammes, A.; Jia, Y.; Wu, Y.; Nguyen, S. T.; Ruoff, R. S. *Carbon N. Y.* **2007**, *45*, 1558–1565.

[34] Pham, V. H.; Cuong, T. V.; Hur, S. H.; Oh, E.; Kim, E. J.; Shin, E. W.; Chung, J. S. *J. Mater. Chem.* **2011**, *21*, 3371–3377.

[35] Qian, Z.; Wang, C.; Du, G.; Zhou, J.; Chen, C.; Ma, J.; Chen, J.; Feng, H. *Cryst. Eng. Comm.* **2012**, *14*, 4976–4979.

[36] Qian, Z.; Zhou, J.; Chen, J.; Wang, C.; Chen, C.; Feng, H. *J. Mater. Chem.* **2011**, *21*, 17635–17637.

[37] Becerril, H. A.; Mao, J.; Liu, Z.; Stoltenberg, R. M., Bao, Z.; Chen, Y. *ACS Nano* **2008**, *2*, 463–470.

[38] Zheng, Q.; Li, Z.; Yang, J.; Kim, J. K. *Prog. Mater. Sci.* **2014**, *64*, 200–247.

[39] Li, L.; Jacobs, D. L.; Bunes, B. R.; Huang, H.; Yang, X.; Zang, L. *Polym. Chem.* **2014**, *5*, 309–313.

[40] Li, S. S.; Tu, K. H.; Lin, C. C.; Chen, C. W.; Chhowalla, M. *ACS Nano* **2010**, *4*, 3169–3174.

[41] Zhang, Y.; Li, L.; Yuan, S.; Li, G.; Zhang, W. *Electrochim. Acta* **2013**, *109*, 221–225.

[42] Kim, H.; So, W.; Moon, S. *Journal of the Korean Physical Society* **2006**, *48*, 441–445.

[43] Zhao, Y.; Yuan, G.; Roche, P.; Leclerc, M. *Polymer* **1995**, *36*, 2211–2214.

[44] Huang, C. PhD, Georgia Institute of Technology, Atlanta, GA, USA, 2010.